Supplemental material

Ye et al., https://doi.org/10.1083/jcb.201709041

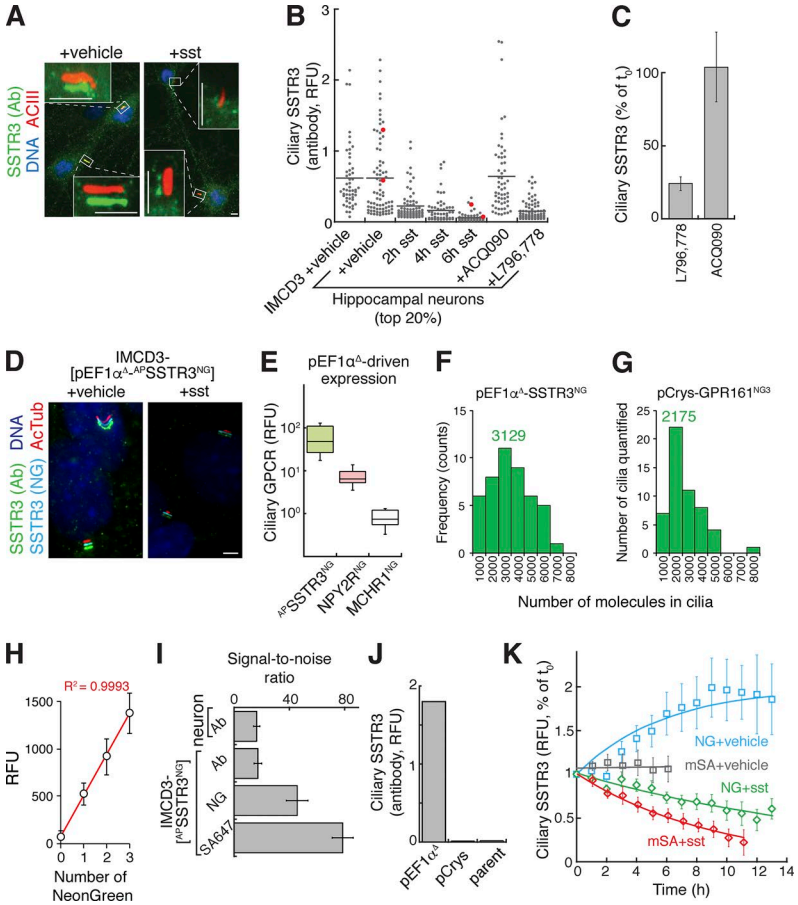

Figure S1. **Low-expression promoters recapitulate the physiological exit kinetics of SSTR3. (A)** Immunofluorescence of rat hippocampal neurons after 6 h treatment with 10 µM sst or vehicle. Cells were stained with antibodies against adenylate cyclase 3 (ACIII) and SSTR3. Channels within insets are shifted. **(B)** Immunofluorescence measurements of SSTR3 levels in individual cilia from rat hippocampal neurons or IMCD3-[pEF1αΔ-^{AP}SSTR3^{NG}] cells. In neuronal cultures, only 20% of cells appeared to express SSTR3 as judged by immunostaining for SSTR3. Therefore, only the 20% brightest cilia in the SSTR3 channel were plotted for each subsequent time point. In IMCD3-[pEF1αΔ-^{AP}SSTR3^{NG}] cells, all cilia were positive for SSTR3 by immunostaining. A horizontal line marks the mean for each condition. Red dots correspond with the cells shown in A. *n* = 52–424 cilia. **(C)** The amount of SSTR3 remaining in cilia after 6 h treatment with the SSTR3-specific agonist L796,778 or SSTR3-specific antagonist ACQ090 was quantified as in B. Error bars represent 95% CI. *n* = 280–424 cilia. **(D)** IMCD3-[pEF1αΔ-^{AP}SSTR3^{NG}] were treated for 6 h with either sst or vehicle. Cells were stained with antibodies against acetylated tubulin (AcTub) and SSTR3 (Ab). In addition, ^{AP}SSTR3^{NG} was visualized by direct fluorescence of NG. Cells were pretreated with the translation inhibitor emetine to eliminate signals from new protein synthesis. Bars, 4 µm. Channels are shifted. **(E)** pEF1αΔ-driven expression produces low levels of ciliary GPCRs. ^{AP}SSTR3^{NG}, NPY2R^{NG}, and MCHR1^{NG} were stably expressed in IMCD3 FlpIn cells. The box plots show the NG intensity measured by live-cell TIRF imaging. The numbers of NPY2R^{NG} and MCHR1^{NG} molecules per cilia are calculated to be 295 and 43 molecules, respectively. *n* = 15–20 cilia. **(F)** Distribution of the absolute number of ^{AP}SSTR3^{NG} per cilia. IMCD3-[pEF1αΔ-^{AP}SSTR3^{NG}] cells were serum starved for 18 h, the ciliary fluorescence intensities were measured and background subtracted, and molecules were counted as detailed in Materials and methods. *n* = 57 cilia. **(G)** Distribution of the absolute number of ^{AP}GPR161^{NG3} per cilia. IMCD3-[pCrys-^{AP}GPR161^{NG3}] cells were serum starved for 18 h, the ciliary fluorescence intensities were measured and background subtracted, and molecules were counted as detailed in Materials and methods. *n* = 53 cilia. **(H)** Validation of sCMOS linearity with NG trimers. Fluorescence intensities from 0, 1, 2, and 3 NG proteins were collected by imaging three-step photobleaching of NG trimers. The red line shows the linear regression curve, and the R^2 value for the linear regression is displayed in the plot. Error bars represent SD. *n* = 5 NG trimers. **(I)** Limited sensitivity of SSTR3 immunostaining. Bars represent measurements of signal/noise ratio of SSTR3 ciliary levels by different modalities. Signal to noise ratio is defined as mean(signal) − mean(background)/SD(background). Ab indicates antibody-based immunofluorescence measurements in fixed cells quantified as in B. NG and mSA647 measurements were conducted by live-cell imaging of IMCD3-[pEF1αΔ-^{AP}SSTR3^{NG}] as in Fig. 1 F. Error bars represent the propagated error. *n* = 14–52 cilia. **(J)** Immunostaining fails to detect low concentrations of SSTR3. IMCD3[pEF1αΔ-^{AP}SSTR3^{GFP}], IMCD3[pCrys-^{AP}SSTR3^{GFP}], and parental IMCD3 cells (which do not express SSTR3 endogenously) were immunostained for SSTR3, and ciliary levels of SSTR3 were measured. *n* = 36–45 cilia. **(K)** Kinetics of ^{AP}SSTR3^{NG} removal. IMCD3-[pEF1αΔ-^{AP}SSTR3^{NG}] cells were pulse-labeled with mSA647 and imaged every hour in the NG and mSA647 channels after addition of vehicle or sst. Imaging NG resulted in a slower apparent removal rate than imaging the same cilia by a mSA647 pulse as the ciliary NG signal is influenced by both import of newly synthesized ^{AP}SSTR3^{NG} and export of ^{AP}SSTR3^{NG} out of cilia; meanwhile, mSA647 pulse-labeled ^{AP}SSTR3^{NG} only reports the ciliary export. Error bars represent SEM. *n* = 10–13 cilia.

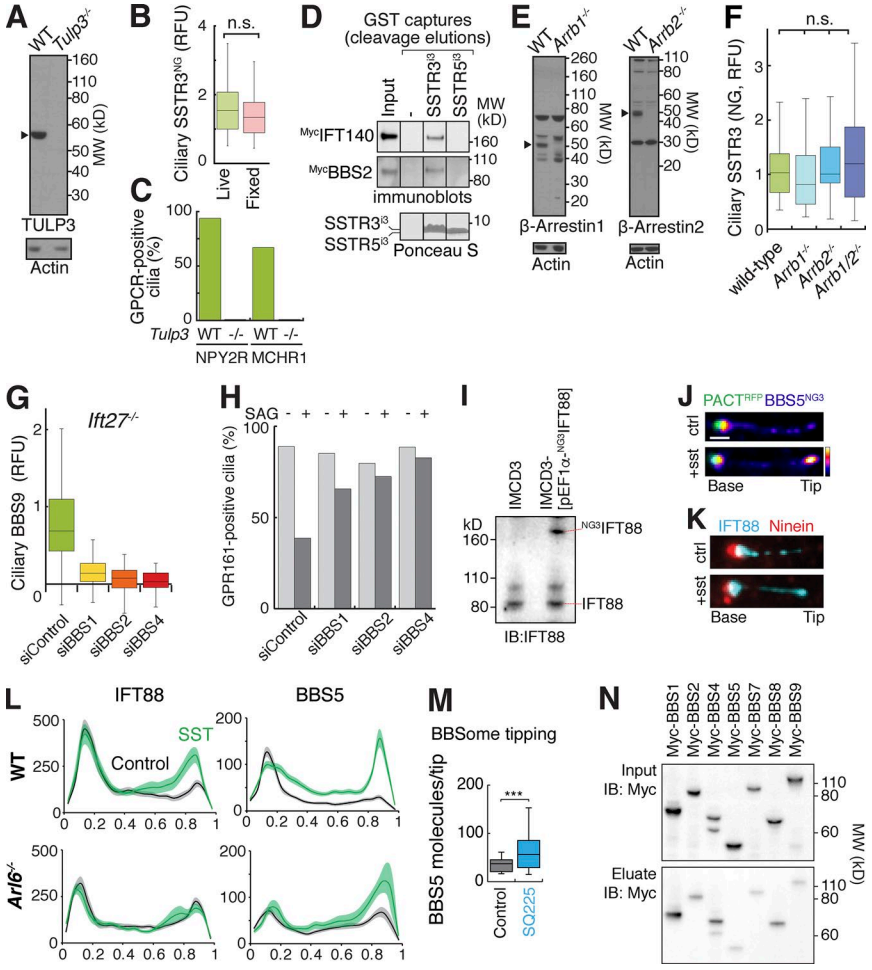

Figure S2. **Molecular requirement for ciliary entry and exit. (A)** Immunoblots of IMCD3 clones knocked out for *Tulp3* by CRISPR/Cas9. Actin was used as a loading control. The immunoblotted antigen is shown below the blot. **(B)** Box plots of ciliary NG fluorescence intensities for IMCD3-[pEF1αΔ-^{AP}SSTR3^{NG}] cells imaged live or after fixation. No significant difference was detected by a *t* test. *n* = 27–59 cilia. **(C)** Ciliary localization of NPY2R^{NG} and MCHR1^{NG} requires Tulp3. The number of NG-positive cilia was counted for WT and *Tulp3*$^{-/-}$ cells by TIRF imaging of fixed cells. Cilia were identified by immunostaining for acetylated tubulin. *n* = 63–91 cilia. **(D)** Capture of IFT-A and BBSome subunits by recombinant GST-SSTR3^{i3}. HEK293 cells were transfected with either ^{Myc}IFT140 or ^{Myc}BBS2. GST-SSTR3^{i3} and GST-SSTR5^{i3} were expressed and purified from *E. coli*. HEK293 extracts were applied to GST-SSTR3^{i3}– and GST-SSTR5^{i3}–coated beads, captured material was eluted by cleavage with PreScission protease, and the resulting eluates were analyzed by Ponceau S and immunoblotting for Myc-tagged subunits. Molecular weights (MWs; kD) are indicated on the right. 10 input equivalents were loaded in the eluate lanes. **(E)** Immunoblots of IMCD3 clones knocked out for β-arrestin 1 (*Arrb1*) or β-arrestin 2 (*Arrb2*) by CRISPR/Cas9. Actin was used as a loading control. The immunoblotted antigen is shown below the blot. **(F)** β-Arrestin 1 and 2 are not required for the accumulation of SSTR3 in cilia. Ciliary ^{AP}SSTR3^{NG} intensities were measured by NG fluorescence (RFUs) for various IMCD3 lines as in Fig. 2 A. All cells were imaged live as cilia were readily identified in the NG channel. n.s. indicates ANOVA significance values where P > 0.05. *n* = 31–59 cilia. **(G)** siRNA knockdown of BBSome subunits was assessed by measuring ciliary BBSome intensities in *Ift27*$^{-/-}$ IMCD3 cells. *Ift27* deletion greatly increases the ciliary abundance of endogenous BBSome (Eguether et al., 2014; Liew et al., 2014), thus facilitating detection of the ciliary BBSome by immunostaining. Cells were treated with either control siRNA or siRNA against BBS1, BBS2, or BBS4 for 48 h, and then cells were serum starved for 24 h, fixed, and stained for endogenous BBS9. *n* = 50–67 cilia. **(H)** The BBSome is necessary for retrieval of GPR161 after Hedgehog pathway activation. BBSome subunits were depleted by siRNA as in G. Cells were then treated with blebbistatin to block ectocytosis-mediated exit (Nager et al., 2017) and with either SAG or vehicle for 2 h, and then cells were fixed and immunostained for GPR161. *n* = 29–96 cilia. **(I)** Relative expression levels of ^{NG3}IFT88. Lysates of IMCD3 and IMCD3-[pEF1α-^{NG3}IFT88] cells were blotted for IFT88. Molecular weights (kD) are indicated on the left. Measurement of band intensities with Image Lab indicates that the molar ratio between ^{NG3}IFT88 and endogenous IFT88 is 1.04. **(J)** The signal-dependent BBSome accumulation at the ciliary tip depicted in Fig. 3 B is shown with the centrosome marker PACT^{RFP} that was transiently expressed to mark the ciliary base (green). Bar, 2 µm. **(K)** Signal-dependent accumulation of IFT-B at the ciliary tip. IMCD3-[pEF1αΔ-^{AP}SSTR3; pEF1α-^{NG3}IFT88] was treated with sst or vehicle for 1 h. Cells were fixed and stained for ninein to mark the basal body, and ^{NG3}IFT88 was imaged by direct NG fluorescence. **(L)** Arl6 is required for the signal-dependent accumulation of IFT-B but not BBSome at the tip of cilia. Line scans of ^{NG3}BBS5 or ^{NG3}IFT88 fluorescence intensities along cilia of live cells. The line marks the mean intensity along length-normalized cilia. The shaded area shows the 95% CI. *n* = 16–32 length-normalized cilia. **(M)** Quantitation of ^{NG3}BBS5 tip fluorescence. ^{NG3}BBS5 tip fluorescence was measured in live IMCD3-[pEF1αΔ-^{AP}SSTR3, pEF1α-^{NG3}BBS5] cells after the indicated drug treatments (as described in Materials and methods). The total number of BBS5 molecules at the tip was calculated using the NG3 calibrator and the measured ratio of ^{NG3}BBS5 to total BBS5. SQ225 is an AC6 inhibitor. Asterisks indicate Mann-Whitney test significance values. ***, P < 0.0005. *n* = 20–29 cilia from three independent experiments. **(N)** Kif7 interacts with BBSome. Cell lysates of HEK293 cells cotransfected with Kif7^{GFP} and individual Myc-tagged BBSome subunits were subjected to immunoprecipitation with anti-GFP antibodies. Lysates and eluates were blotted for Myc. Molecular weights (kD) are indicated on the right.

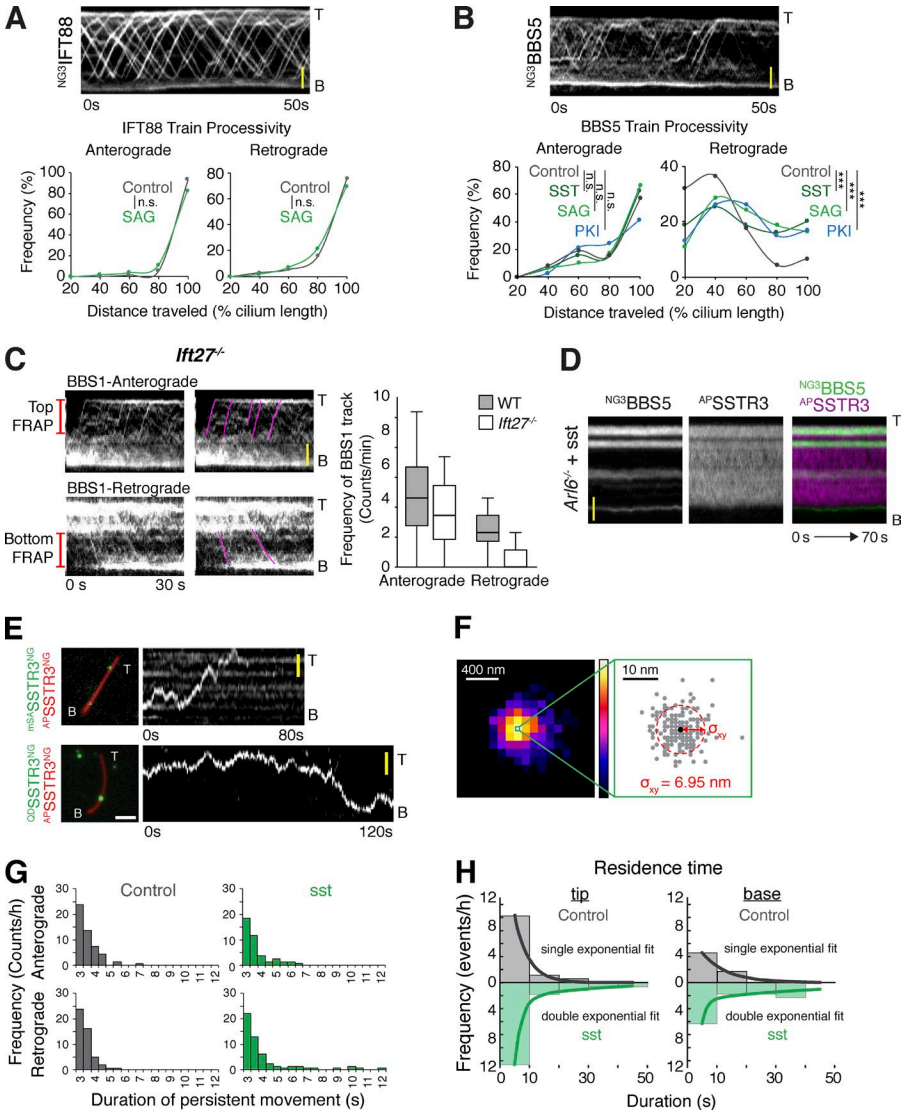

Figure S3. **BBS5/IFT88 train processivity and single-molecule quantitation. (A)** Top: Representative kymograph from IMCD3-[pEF1α-^{NG3}IFT88] cells showing the highly processive movement of IFT-B trains. Bottom: Distribution of the processivity of IFT-B trains. The processivity of IFT-B trains was measured in IMCD3-[pEF1α-^{NG3}IFT88] cells as described in Fig. 5 A. Significance value of Mann-Whitney test applied to the entire distribution. n.s., $P > 0.05$. B, base; T, tip. **(B)** Top: Representative kymograph from IMCD3-[pEF1α-^{NG3}BBS5] cells showing the movement of BBSome trains. Bottom: Distribution of the processivity of BBSome trains. IMCD3-[pEF1α-^{NG3}BBS5] cells were treated with vehicle, sst, SAG, or PKI for 40 min before imaging. Processivity was scored as described in Fig. 6 C. Asterisks indicate the significance values of Mann-Whitney tests applied to the entire distribution. n.s., $P > 0.1$; ***, $P < 0.0005$. **(C)** Ift27 is required for the assembly of processive retrograde BBSome trains. Left: Representative kymographs from *Ift27*$^{-/-}$ IMCD3-[pEF1α-^{NG3}BBS1] cilia. To overcome the difficulties in visualizing BBSome trains in cilia of *Ift27*$^{-/-}$ cells where the levels of BBSome are fourfold elevated compared with WT cells (Liew et al., 2014), one half of the ciliary ^{NG3}BBS1 fluorescent signal was photobleached, and the trains entering the bleached area were imaged and counted. The red lines mark areas photobleached at t_0. The anterograde or retrograde BBSome trains entering the photobleached areas are highlighted with magenta lines. Right: The frequency of highly processive BBSome trains in WT or *Ift27*$^{-/-}$ cells was graphed. Error bars represent SEM. n = 23–37 cilia from three independent experiments. **(D)** Arl6 is required for the assembly of cargo-laden BBSome retrograde trains. Kymographs showing BBSome and SSTR3 foci in cilia of *Arl6*$^{-/-}$ cells. mSA647-labeled IMCD3-[pEF1αΔ-^{AP}SSTR3, pEF1α-^{NG3}BBS5] cells were treated with sst for 1 h before imaging at 1.21 Hz. The cells stably expressed an ER-localized biotin ligase BirA to enable visualization of ^{AP}SSTR3 by mSA647 labeling. Channels are shown individually and merged. In this kymograph, BBSome and SSTR3 stay in immobile foci near the tip of cilia. In some *Arl6*$^{-/-}$ cilia such as the one shown in Fig. 7 E, the large accumulations of BBSomes at the tip occasionally gave rise to retrograde trains. In neither kymographs were retrograde tracks of SSTR3 detected. **(E)** Representative kymographs showing the diffusive behavior of mSA647-labeled ^{AP}SSTR3^{NG} (top) and QDot655-labeled ^{AP}SSTR3^{NG} (bottom) in the absence of sst. Bars, 2 µm. **(F)** Localization precision of Qdot655. Left: A representative fluorescence image from a single Qdot655 emitter immobilized on the glass coverslip. Intensities are presented in fire scale. Right: Repeated acquisitions of the same Qdot655 over time were used to map the centroid of fluorescence (gray dots) and to calculate the lateral localization precision σ_{xy} as described by Deschout et al. (2014). **(G)** Durations of persistent movement events of single molecules of ^{QD}SSTR3 in anterograde and retrograde directions. n = 77–82 persistent movement events. **(H)** Durations of residence events for ^{QD}SSTR3 at ciliary tip or base. For visualization, data were fitted as indicated to either a single or a double exponential. n = 11–28 residence events quantified from 24 cilia.

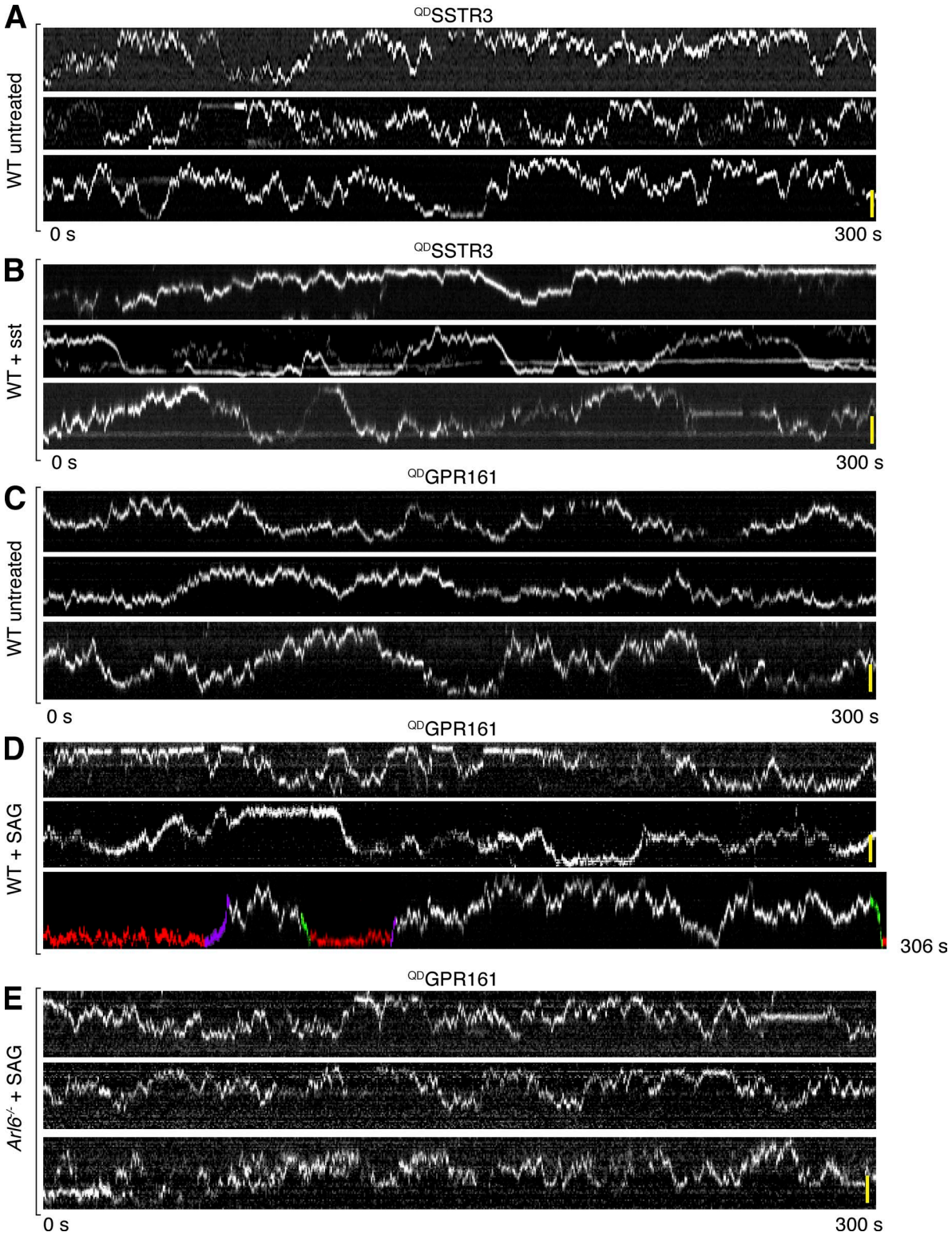

Figure S4. **Kymographs of single molecules of ^{QD}SSTR3 and ^{QD}GPR161. (A and B)** Additional examples of ^{QD}SSTR3 tracking in WT cells treated with either vehicle or sst. Each kymograph shows a single cilium that was tracked for 5 min. **(C–E)** Additional examples of ^{QD}GPR161 tracking in either WT or *Arl6*$^{-/-}$ cells treated with either vehicle or SAG. Bars, 2 µm. Each kymograph shows a single cilium that was tracked for 5 min. The annotated kymograph shown in D corresponds with the kymograph shown in Fig. 9 A.

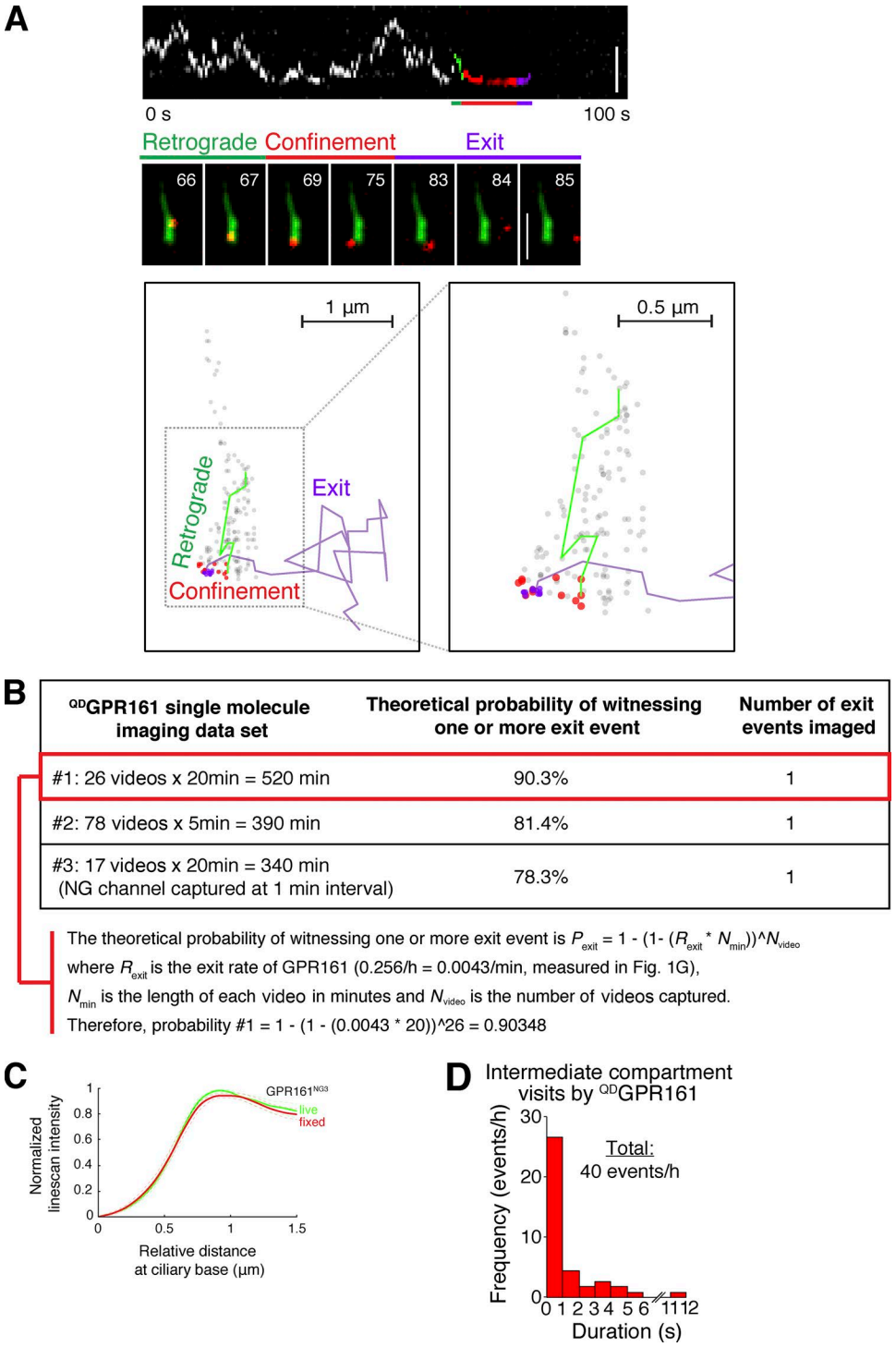

QDGPR161 single molecule imaging data set	Theoretical probability of witnessing one or more exit event	Number of exit events imaged
#1: 26 videos x 20min = 520 min	90.3%	1
#2: 78 videos x 5min = 390 min	81.4%	1
#3: 17 videos x 20min = 340 min (NG channel captured at 1 min interval)	78.3%	1

The theoretical probability of witnessing one or more exit event is $P_{exit} = 1 - (1- (R_{exit} * N_{min}))^N_{video}$
where R_{exit} is the exit rate of GPR161 (0.256/h = 0.0043/min, measured in Fig. 1G),
N_{min} is the length of each video in minutes and N_{video} is the number of videos captured.
Therefore, probability #1 = 1 - (1 - (0.0043 * 20))^26 = 0.90348

Figure S5. **Visualization of QDGPR161 exit at single-molecule resolution. (A)** Exit event observed from QDGPR161 single-molecule tracking. Cells were treated with SAG for 40 min before the start of imaging. Green, red, and purple labels in the kymograph (top) and line coloring in time lapse images (middle) indicate retrograde movements, confinement, and exit from cilia, respectively. Bottom: Centroid mapping of QDGPR161. Bars (unless otherwise indicated), 2 µm. **(B)** The frequency of GPR161 exit events captured by single-molecule imaging is consistent with values predicted from bulk imaging of APGPR161NG3. Single-molecule imaging videos are grouped into three datasets, each with slightly different acquisition settings. The theoretical probability of witnessing one or more exit event is $P_{exit} = 1 - (1 - (R_{exit} * N_{min}))^N_{video}$, where R_{exit} is the exit rate of GPR161 (0.256/h = 0.0043/min; measured in Fig. 1 G), N_{min} is the length of each video in minutes, and N_{video} is the number of videos captured. **(C)** Longitudinal scans of APGPR161NG3 fluorescence in live cells (green line) and fixed cells (red line). Dotted lines represent 95% CI. *n* = 20–28 cilia. **(D)** Distribution of intermediate compartment visit durations for a single molecule of QDGPR161. IMCD3 cells were treated with SAG for 40 min before imaging each cilium for 5–10 min. Intermediate compartment visits are defined by the centroid of QDGPR161 crossing the 50th percentile of bulk NG fluorescence of APGPR161NG3. Combined imaging time was 70 min. *n* = 45 intermediate compartment visits.

wild-type cells

image SA647
pulse-labeled SSTR3

1 frame per hour

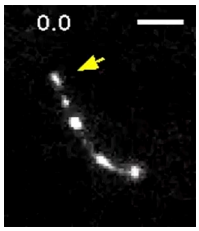

Video 1. **Sst-dependent removal of SSTR3 from cilia.** Live-cell imaging of $SSTR3^{NG}$ after addition of sst. IMCD3-[pEF1αΔ-$^{AP}SSTR3^{NG}$] cells were pulse-labeled by mSA647, and cilia were tracked for 2 or 6 h after addition of sst or vehicle. The fluorescence is displayed in fire color scale. Time stamp is in h:min:s. Video is played back at two frames per second. Bar, 4 µm.

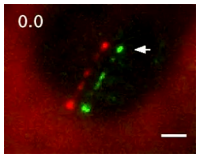

Video 2. **IFT-B foci movements in cilia.** Live imaging of ^{NG3}IFT88 in IMCD3-[pEF1α-^{NG3}IFT88] cells. An arrow marks the tip of the cilium. Time stamp is in seconds. Video is played back at 10 frames per second. Bar, 2 µm.

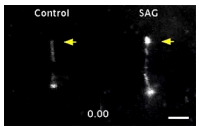

Video 3. **Comovement of BBSome and IFT-B.** Live-cell imaging showing BBSome (green) and IFT-B (red) foci comoving in IMCD3-[pEF1α-^{NG3}BBS1, pCMV-^{tdTomato}IFT88] cells. Channels are shifted to aid visualization. An arrow marks the tip of the cilium. Time stamp is in seconds. Video is played back at 10 frames per second. Bar, 2 µm.

Video 4. **BBSome foci movement in cilia.** Live imaging of ^{NG3}BBS5 in IMCD3-[pEF1α-^{NG3}BBS5] cells treated with vehicle or SAG for 40 min. Arrows mark the cilium tips. A bright retrograde BBSome focus is seen in the SAG-treated cell between 12.0 and 15.0 s. Time stamp is in seconds. Video is played back at 10 frames per second. Bar, 2 µm.

wild type cells
pretreated with somatostatin
for 1 hour

co-image SSTR3 and BBSome
high frequency imaging

Video 5. **Dynamics of BBSome-mediated retrieval.** Live-cell imaging of BBSome foci and SSTR3 in WT and *Arl6*$^{-/-}$ cells. IMCD3-[^{AP}SSTR3, ^{NG3}BBS5] were pulse-labeled with mSA647 and treated with sst for 1 h before imaging at 1.21 Hz. Channels are shifted to aid visualization. Yellow and red arrowheads point to the base and tip of cilia, respectively. Time stamp is in min:s. Video is played back at 12 frames per second. Bar, 4 µm.

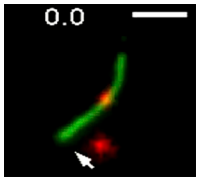

Video 6. **Behavior of Qdot-labeled SSTR3 in control-treated cells.** Single-molecule imaging of SSTR3 in an IMCD3-[pEF1αΔ-$^{AP}SSTR3^{NG}$] cell. SSTR3 was sparsely labeled with Qdot655 (^{QD}SSTR3, red channel) and tracked as detailed in the Materials and methods. The bulk NG fluorescence from $^{AP}SSTR3^{NG}$ is shown in the green channel. An arrow marks the base of the cilium. Time stamp is in seconds. Video is played back at 20 frames per second. Bar, 2 µm.

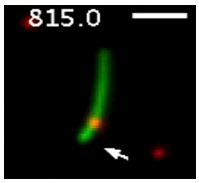

Video 7. **Behavior of Qdot-labeled SSTR3 in sst-treated cells.** Single-molecule imaging of SSTR3 in an sst-treated IMCD3-[pEF1αΔ-$^{AP}SSTR3^{NG}$] cell. SSTR3 was sparsely labeled with Qdot655 (^{QD}SSTR3, red channel) and tracked as detailed in the Materials and methods. The cell was treated with sst for >1 h before imaging. The bulk NG fluorescence from $^{AP}SSTR3^{NG}$ is shown in the green channel. An arrow marks the base of the cilium. Time stamp is in seconds. Video is played back at 10 frames per second. Bar, 2 µm.

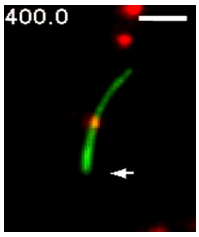

Video 8. **Direct observation of ciliary exit of Qdot-labeled GPR161.** Single-molecule imaging of GPR161 exit in a SAG-treated IMCD3-[pCrys-^{AP}GPR161^{NG3}] cell. GPR161 was sparsely labeled with Qdot655 (^{QD}GPR161, red channel) and tracked as detailed in Materials and methods. The cell was treated with SAG for >1 h before imaging. The bulk NG fluorescence from ^{AP}SSTR3^{NG} is shown in the green channel. An arrow marks the base of cilium. Time stamp is in seconds. Video is played back at 20 frames per second. Bar, 2 µm.

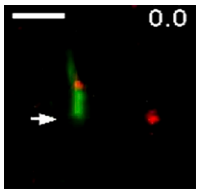

Video 9. **Direct observation of ciliary exit of Qdot-labeled GPR161.** Single-molecule imaging of GPR161 exit in a SAG-treated IMCD3-[pCrys-^{AP}GPR161^{NG3}] cell. GPR161 was sparsely labeled with Qdot655 (^{QD}GPR161, red channel) and tracked as detailed in Materials and methods. The cell was treated with SAG for >1 h before imaging. The bulk NG fluorescence from ^{AP}SSTR3^{NG} is shown in the green channel. An arrow marks the base of cilium. Time stamp is in seconds. Video is played back at 20 frames per second. Bar, 2 µm.

References

Deschout, H., F. Cella Zanacchi, M. Mlodzianoski, A. Diaspro, J. Bewersdorf, S.T. Hess, and K. Braeckmans. 2014. Precisely and accurately localizing single emitters in fluorescence microscopy. *Nat. Methods.* 11:253–266. https://doi.org/10.1038/nmeth.2843

Eguether, T., J.T. San Agustin, B.T. Keady, J.A. Jonassen, Y. Liang, R. Francis, K. Tobita, C.A. Johnson, Z.A. Abdelhamed, C.W. Lo, and G.J. Pazour. 2014. IFT27 links the BBSome to IFT for maintenance of the ciliary signaling compartment. *Dev. Cell.* 31:279–290. https://doi.org/10.1016/j.devcel.2014.09.011

Liew, G.M., F. Ye, A.R. Nager, J.P. Murphy, J.S. Lee, M. Aguiar, D.K. Breslow, S.P. Gygi, and M.V. Nachury. 2014. The intraflagellar transport protein IFT27 promotes BBSome exit from cilia through the GTPase ARL6/BBS3. *Dev. Cell.* 31:265–278. https://doi.org/10.1016/j.devcel.2014.09.004

Nager, A.R., J.S. Goldstein, V. Herranz-Pérez, D. Portran, F. Ye, J.M. Garcia-Verdugo, and M.V. Nachury. 2017. An Actin Network Dispatches Ciliary GPCRs into Extracellular Vesicles to Modulate Signaling. *Cell.* 168:252–263. https://doi.org/10.1016/j.cell.2016.11.036